Characterizing and Adapting to the Structure of Millimeter Wave Channel Covariance Matrices

Dennis Ogbe*, Vasanthan Raghavan†, David J. Love*
*Purdue University, West Lafayette, IN 47907, USA
†Qualcomm, Inc., Bridgewater, NJ 08807, USA
E-mail: dogbe@purdue.edu, vasanthan_raghavan@ieee.org, djlove@purdue.edu

***Abstract*—We consider the classical estimation-theoretic framework of a channel estimation phase followed by a data transmission phase for a class of widely-used millimeter wave (mmW) channel models. We derive the structure of optimal transmissions/sounding beams during the channel estimation phase and show that this structure depends on the transmit covariance matrix of the channel. To further understand this structure, we derive exact and approximate expressions for the transmit and receive covariance matrices of the channel. We conclude the paper with numerical studies on the accuracy of our approximations and apply the results of our analysis to the problem of the energy trade-off between the channel estimation and data transmission phases.**

I. Introduction

Wireless communications in the millimeter wave (mmW) spectrum is considered to be a key enabler in bridging the burgeoning gap between exponentially increasing wireless data traffic and the limited supply of electromagnetic spectrum available for communications [1]–[5]. Millimeter wave systems, by virtue of operating with center frequencies in the (approximately) 24–300 GHz range, have exposed communication engineers to a unique set of technical challenges in overcoming the increased free-space propagation, material penetration and blockage losses in this frequency regime.

The most popular approach to solve this problem involves the use of a large number of antennas at the transmitter as well as the receiver. While these multiple-input multiple-output (MIMO) architectures are common at traditional sub-6 GHz frequencies, applying tried-and-tested ideas from the MIMO literature to mmW systems poses significant additional challenges, mainly due to the increased cost and complexity in manufacturing/processing nodes and the high-power consumption of the components of the radio-frequency (RF) chain (e.g., analog-to-digital converters, transmit and receive filters, amplifiers, mixers, etc.). These challenges together with the expectation that the number of antennas for mmW will greatly exceed the number of antennas for sub-6 GHz systems, have led communication engineers to explore the lower complexity *analog* beamforming approach, which requires a smaller number of RF chains [6]–[11].

The focus of this work is on studying the mmW beam sounding design problem from an estimation-theoretic perspective hitherto applied to sub-6 GHz systems. In Sec. II, we briefly present a practical and commonly-used mmW channel model with some model parameters motivated by real-world cellular deployments. In Sec. III, we derive the structure of the optimal transmissions using a classical minimum mean squared error (MMSE) estimation setup. Motivated by these results, we then derive exact and approximate expressions for the transmit and receive covariance matrices with the assumed channel model. In Sec. IV, we numerically study the accuracy of our approximate expressions and use these expressions to investigate the trade-off between channel estimation and data transmission given a fixed energy budget. These results complement similar studies traditionally performed in the sub-6 GHz regime [12]–[15].

Notations: Lower- ($\mathbf{x}$) and upper-case block ($\mathbf{X}$) letters denote vectors and matrices with $\mathbf{x}(i)$ and $\mathbf{X}(i,j)$ denoting the i-th and (i,j)-th entries of $\mathbf{x}$ and $\mathbf{X}$, respectively. $\|\mathbf{x}\|_2$ denotes the ℓ_2-norm of a vector $\mathbf{x}$, whereas $\mathbf{x}^\dagger$, $\mathbf{x}^T$ and $\mathbf{x}^\star$ denote the complex conjugate Hermitian transpose, regular transpose and complex conjugation operations of $\mathbf{x}$, respectively. We use $\mathbb{C}$ to denote the field of complex numbers and $\mathcal{E}$ to denote the expectation operation.

II. Channel Model

We consider a single-user millimeter wave setting with a multi-antenna transmitter serving a multi-antenna receiver. The transmitter and receiver are assumed to be equipped with planar arrays of $N_{\mathsf{tx}} \times N_{\mathsf{tz}}$ antennas and $N_{\mathsf{rx}} \times N_{\mathsf{rz}}$ antennas, respectively. At both ends, the inter-antenna element spacing is $\lambda/2$ where λ is the wavelength of propagation. With $N_t = N_{\mathsf{tx}}N_{\mathsf{tz}}$ and $N_r = N_{\mathsf{rx}}N_{\mathsf{rz}}$, the channel $\mathbf{H} \in \mathbb{C}^{N_r \times N_t}$ between the transmitter and the receiver is given by an extended geometric propagation model over L clusters/paths [16]:

$$\mathbf{H} = \sqrt{\frac{N_r N_t}{L}} \sum_{\ell=1}^{L} \alpha_\ell \, \mathbf{u}_\ell \, \mathbf{v}_\ell^\dagger . \tag{1}$$

In (1), α_ℓ, $\mathbf{u}_\ell$ and $\mathbf{v}_\ell$ denote the complex path gain, and the unit-norm array steering vectors at the receiver and transmitter ends, respectively. The path gains are assumed to be independent of the steering vectors and are modeled as independent and identically distributed (i.i.d.) standard complex Gaussian random variables: $\alpha_\ell \sim \mathcal{CN}(0,1)$. The array steering vectors, $\mathbf{u}_\ell$ and $\mathbf{v}_\ell$, depend on the angle of arrival (AoA) and the angle of departure (AoD) in azimuth and zenith from the cluster to the receiver and from the transmitter to the cluster, respectively. The k-th entries of $\mathbf{u}_\ell$ and $\mathbf{v}_\ell$ are given as [17]:

$$\mathbf{u}_\ell(k) = \frac{1}{\sqrt{N_r}} \cdot e^{j\pi(m \cdot \sin(\theta_{\mathsf{R},\ell}) \cos(\phi_{\mathsf{R},\ell}) + n \cdot \cos(\theta_{\mathsf{R},\ell}))}$$

for $0 \leq m \leq N_{\mathsf{rx}} - 1$, $0 \leq n \leq N_{\mathsf{rz}} - 1$, and $k = mN_{\mathsf{rz}} + n + 1$, and

$$\mathbf{v}_\ell(k) = \frac{1}{\sqrt{N_t}} \cdot e^{j\pi(m \cdot \sin(\theta_{\mathsf{T},\ell}) \cos(\phi_{\mathsf{T},\ell}) + n \cdot \cos(\theta_{\mathsf{T},\ell}))},$$

for $0 \leq m \leq N_{\mathsf{tx}} - 1$, $0 \leq n \leq N_{\mathsf{tz}} - 1$, and $k = mN_{\mathsf{tz}} + n + 1$, where $\phi_{\mathsf{R},\ell}$ and $\phi_{\mathsf{T},\ell}$ denote the AoA/AoD in azimuth, and $\theta_{\mathsf{R},\ell}$ and $\theta_{\mathsf{T},\ell}$ denote the AoA/AoD in elevation, all for the ℓ-th cluster, respectively.

We furthermore assume that $\phi_{\mathsf{R},\ell}$, $\theta_{\mathsf{R},\ell}$, $\phi_{\mathsf{T},\ell}$ and $\theta_{\mathsf{T},\ell}$ are uniformly distributed over a certain angular spread (denoted as α_{R}, β_{R}, α_{T} and β_{T}, respectively) around a certain cluster angle (denoted as $\overline{\phi}_{\mathsf{R}}$, $\overline{\theta}_{\mathsf{R}}$, $\overline{\phi}_{\mathsf{T}}$ and $\overline{\theta}_{\mathsf{T}}$, respectively). This assumption makes sense in the downlink setting with practical base-station deployments tailored for a certain elevation downtilt and a sectored coverage. Reasonable model parameters in this scenario include $\overline{\phi}_{\mathsf{T}} = 0°$ (without loss in generality), $\overline{\theta}_{\mathsf{T}} = 90\text{-}110°$, an azimuth coverage of $\alpha_{\mathsf{T}} = 90\text{-}120°$, and an elevation coverage of $\beta_{\mathsf{T}} = 0\text{-}45°$. For the uplink setting, at the user end, since the antenna array(s) are expected to provide full coverage over the sphere, it does not make sense to restrict $\overline{\phi}_{\mathsf{R}}$, $\overline{\theta}_{\mathsf{R}}$, α_{R} or β_{R}.

III. Optimal Sounding Beam Design

In this section, we pose a classical channel estimation problem using the model from Sec. II. We then derive the optimal sounding beams as a function of the eigenbasis of the transmit covariance matrix of the channel. We finish the section by deriving exact and approximate expressions for the covariance matrices and comment on their structures.

A. Structure of Optimal Sounding Beams

Let the energy budget for channel estimation be ρ. The input-output model for estimating the downlink channel is then given as

$$\mathbf{Y}_{\mathsf{tr}} = \sqrt{\frac{\rho}{N_t}} \cdot \mathbf{H}\mathbf{X}_{\mathsf{tr}} + \mathbf{N}_{\mathsf{tr}}, \tag{2}$$

where $\mathbf{X}_{\mathsf{tr}}$ is the $N_t \times N_t$-dimensional estimation matrix with $\mathcal{E}\left[\mathsf{Tr}(\mathbf{X}_{\mathsf{tr}}\mathbf{X}_{\mathsf{tr}}^\dagger)\right] \leq N_t$, $\mathbf{H}$ is the $N_r \times N_t$ channel matrix and $\mathbf{N}_{\mathsf{tr}}$ is the additive white Gaussian noise matrix (of size $N_r \times N_t$) with i.i.d. entries distributed as $\mathbf{N}_{\mathsf{tr}}(i,j) \sim \mathcal{CN}(0,1)$. Let the transmit covariance matrix be denoted as $\mathbf{R}_{\mathsf{tx}} = \mathcal{E}\left[\mathbf{H}^\dagger\mathbf{H}\right]$. Proposition 1 establishes the structure of the optimal training matrix $\mathbf{X}_{\mathsf{tr}}$ when performing MMSE estimation.

Proposition 1. *Let the eigen-decomposition of $\mathbf{R}_{\mathsf{tx}}$ be expressed as*

$$\mathbf{R}_{\mathsf{tx}} = \mathbf{U}_{\mathsf{tx}}\mathbf{\Lambda}_{\mathsf{tx}}\mathbf{U}_{\mathsf{tx}}^\dagger. \tag{3}$$

Without loss in generality, let the diagonal entries of $\mathbf{\Lambda}_{\mathsf{tx}}$ be arranged in non-increasing order. The structure of the optimal $\mathbf{X}_{\mathsf{tr}}$ that minimizes the mean squared error for channel estimation is as follows:

$$\mathbf{X}_{\mathsf{tr}} = \mathbf{U}_{\mathsf{tx}}\mathbf{D}_{\mathsf{tx}}, \tag{4}$$

where $\mathbf{D}_{\mathsf{tx}}$ is a diagonal matrix whose diagonal elements $\mathbf{D}_{\mathsf{tx}}(i)$ are chosen via a waterfilling-type procedure over the diagonal entries of $\mathbf{\Lambda}_{\mathsf{tx}}$.

The proof of Prop. 1 follows directly from minimizing the trace of the estimation error covariance matrix and is omitted due to space constraints. The main takeaway from Proposition 1 is that, as expected, the optimal sounding beams are a function of the eigenspace of the transmit covariance matrix $\mathbf{R}_{\mathsf{tx}}$. The structure of $\mathbf{R}_{\mathsf{tx}}$ can thus give us insights on the structure of the optimal sounding beams.

B. Exact and Approximate Expressions for the Transmit and Receive Covariance Matrices

We begin with the exact characterization of the covariance matrices for the channel model and with the assumptions on its parameters from Sec. II.

Proposition 2. *Under the assumptions from Section II, the elements of the transmit covariance matrix $\mathbf{R}_{\mathsf{tx}}$ are of the form given in* (5)*, where*

$$k_1 = m_1 N_{\mathsf{tz}} + n_1 + 1, \quad k_2 = m_2 N_{\mathsf{tz}} + n_2 + 1$$

and $E_0^+(w,z) = \frac{2}{\pi}\int_0^w e^{jz\cos(u)}du$ is the zero-th order incomplete cylindrical function of the Poisson form [18, 1.4, p. 23]. Furthermore, the elements of the receive covariance matrix $\mathbf{R}_{\mathsf{tx}}$ are given in (6)*, where*

$$k_1 = m_1 N_{\mathsf{rz}} + n_1 + 1, \quad k_2 = m_2 N_{\mathsf{rz}} + n_2 + 1,$$

and $J_0(z) = \frac{1}{\pi}\int_0^\pi \cos\left(z\cos(u)\right)du$ is the zero-th order Bessel function of the first kind [19, 9.1.18, p. 360].

Definition 1 (Block Toeplitz matrix)**.** *A block Toeplitz matrix is a block matrix where the blocks are repeated along the diagonals in Toeplitz form, with each block in itself being a Toeplitz matrix.*

Corollary 1. *Both $\mathbf{R}_{\mathsf{tx}}$ and $\mathbf{R}_{\mathsf{rx}}$ are block Toeplitz matrices.*

Proof. Note that

$$\mathcal{E}\left[\mathbf{H}\right] \triangleq \sqrt{\frac{N_r N_t}{L}} \cdot \sum_{\ell=1}^{L} \mathcal{E}\left[\alpha_\ell\right] \cdot \mathcal{E}\left[\mathbf{u}_\ell \mathbf{v}_\ell^\dagger\right] = \mathbf{0},$$

which follows from i) the independence of the AoA/AoD and ii) the path gains and the zero mean of α_ℓ. We start with the

$$\frac{\mathbf{R}_{\mathsf{tx}}(k_1,k_2)}{N_r} = \begin{cases} \frac{\pi}{\alpha_{\mathsf{T}}\beta_{\mathsf{T}}} \cdot \int_{\overline{\theta}_{\mathsf{T}} - \frac{\beta_{\mathsf{T}}}{2}}^{\overline{\theta}_{\mathsf{T}} + \frac{\beta_{\mathsf{T}}}{2}} E_0^+\left(\frac{\alpha_{\mathsf{T}}}{2}, \pi(m_1 - m_2)\sin(\theta)\right) \cdot e^{j\pi(n_1 - n_2)\cos(\theta)}d\theta & \text{if } \beta_{\mathsf{T}} > 0 \\ \frac{\pi}{\alpha_{\mathsf{T}}} \cdot E_0^+\left(\frac{\alpha_{\mathsf{T}}}{2}, \pi(m_1 - m_2)\sin(\overline{\theta}_{\mathsf{T}})\right) \cdot e^{j\pi(n_1 - n_2)\cos(\overline{\theta}_{\mathsf{T}})} & \text{if } \beta_{\mathsf{T}} = 0 \end{cases} \tag{5}$$

$$\frac{\mathbf{R}_{\mathsf{rx}}(k_1,k_2)}{N_t} = J_0\left(\frac{\pi}{2}\left[\sqrt{(m_1 - m_2)^2 + (n_1 - n_2)^2} + (n_1 - n_2)\right]\right) \cdot J_0\left(\frac{\pi}{2}\left[\sqrt{(m_1 - m_2)^2 + (n_1 - n_2)^2} - (n_1 - n_2)\right]\right) \tag{6}$$

transmit covariance matrix. The second moment (as seen from the transmit side) can be defined as

$$\begin{aligned}\mathbf{R}_{\mathsf{tx}} &\triangleq \mathcal{E}\left[\mathbf{H}^{\dagger}\mathbf{H}\right] \\ &= \frac{N_r N_t}{L}\cdot\mathcal{E}\left[\sum_{\ell_1}\sum_{\ell_2}\alpha^{\star}_{\ell_1}\alpha_{\ell_2}\mathbf{v}_{\ell_1}\mathbf{v}^{\dagger}_{\ell_2}\cdot\left(\mathbf{u}^{\dagger}_{\ell_1}\mathbf{u}_{\ell_2}\right)\right].\end{aligned}$$

Using i) the independence of AoA/AoD and path gains ii) the uncorrelated nature and zero mean of α_ℓ, and iii) the unit-norm of $\mathbf{u}_\ell$, we can simplify $\mathbf{R}_{\mathsf{tx}}$ as

$$\begin{aligned}\mathbf{R}_{\mathsf{tx}} &= \frac{N_r N_t}{L}\cdot\sum_{\ell=1}^{L}\mathcal{E}\left[|\alpha_\ell|^2\right]\cdot\mathcal{E}\left[\mathbf{v}_\ell\mathbf{v}^{\dagger}_{\ell}\right] \\ &= \frac{N_r N_t}{L}\cdot\sum_{\ell=1}^{L}\mathcal{E}\left[\mathbf{v}_\ell\mathbf{v}^{\dagger}_{\ell}\right],\end{aligned}$$

where the last step follows from the unit variance of α_ℓ. We now define the functions $F_1(z)$ and $F_2(z)$ as follows:

$$F_1(z) = \int_{\phi\in\Phi_{\mathsf{T}}}\cos\big(z\cos(\phi)\big)f_{\mathsf{T}}(\phi)d\phi, \tag{7}$$

$$F_2(z) = \int_{\phi\in\Phi_{\mathsf{T}}}\sin\big(z\cos(\phi)\big)f_{\mathsf{T}}(\phi)d\phi. \tag{8}$$

Using the identically distributed nature of the AoA/AoDs and the above function definitions, we can write $\mathbf{R}_{\mathsf{tx}}(k_1,k_2)$ as in (9) below, where $k_1 = m_1 N_{\mathsf{tz}} + n_1 + 1$ and $k_2 = m_2 N_{\mathsf{tz}} + n_2 + 1$.

The assumption of uniformly distributed cluster angles leads to further simplifications of (7) and (8). More specifically, we obtain

$$\begin{aligned}F_1(z) &= \frac{1}{\alpha_{\mathsf{T}}}\int_{-\alpha_{\mathsf{T}}/2}^{\alpha_{\mathsf{T}}/2}\cos\left(z\cos(\phi)\right)d\phi \\ &= \frac{2}{\alpha_{\mathsf{T}}}\int_{0}^{\alpha_{\mathsf{T}}/2}\cos\left(z\cos(\phi)\right)d\phi \\ &= \frac{\pi}{\alpha_{\mathsf{T}}}\cdot J_0\left(\frac{\alpha_{\mathsf{T}}}{2},z\right),\end{aligned}$$

for $F_1(z)$, where $J_0(w,z)$ is the incomplete Bessel function [18]. Using a similar analysis for $F_2(z)$, we observe that

$$F_2(z) = \frac{\pi}{\alpha_{\mathsf{T}}}\cdot H_0\left(\frac{\alpha_{\mathsf{T}}}{2},z\right), \tag{10}$$

where $H_0(w,z)$ is the incomplete Struve function. Both $J_0(w,z)$ and $H_0(w,z)$ are generalizations of the *standard* Bessel and Struve functions $J_0(z)$ and $H_0(z)$ and form the real and imaginary parts of the incomplete cylindrical function $E_0^+(w,z)$ [18]. Re-writing (9) in terms of $E_0^+(w,z)$ leads to the expression (5). A similar chain of reasoning can be applied to arrive at (6).

To gain insight into the statement of Corollary 1, we consider the indices in (5) and note that since $k_1 - k_2 = (m_1-m_2)N_{\mathsf{tz}} + n_1 - n_2$, it can be seen that

$$\begin{aligned}n_1 - n_2 &= (k_1-k_2) \bmod N_{\mathsf{tz}} \\ m_1 - m_2 &= \frac{k_1 - k_2 - [(k_1-k_2) \bmod N_{\mathsf{tz}}]}{N_{\mathsf{tz}}}.\end{aligned}$$

Note that different (m_1-m_2, n_1-n_2)-pairs could map to (k_1,k_2)-pairs such that k_1-k_2 are the same. Thus, for fixed values of m_1-m_2, every resulting block depends only on n_1-n_2 and is thus Toeplitz. Furthermore, the blocks itself change as functions of (m_1-m_2), resulting in the aforementioned block Toeplitz structure. ■

We note that special functions like $E_0^+(w,z)$—both standard and incomplete versions—have been of interest in electromagnetic theory for a long time; see, e.g., [17], [20], [21] and references therein. Thus, it is not surprising to see such functions in channel modeling applications. More recently, such functions have been useful in problems in communication theory.

To close this section, we note that while (5) and (6) provide exact expressions for the transmit and receive covariance matrices, the complicated nature of special functions like $E_0^+(w,z)$ renders these expressions difficult to handle for further analysis or implementation. To overcome this difficulty, Prop. 3 provides some intuition on the behavior of the entries of $\mathbf{R}_{\mathsf{tx}}$ and $\mathbf{R}_{\mathsf{rx}}$ as the antenna dimentions increase. The numerical studies in Sec. IV-A will study the accuracy of these approximations.

Proposition 3. *If $m_1 = m_2$, we have*

$$\frac{\mathbf{R}_{\mathsf{tx}}(k_1,k_2)}{N_r} = \begin{cases}\frac{1}{\beta_{\mathsf{T}}}\int_{\overline{\theta}_{\mathsf{T}}-\frac{\beta_{\mathsf{T}}}{2}}^{\overline{\theta}_{\mathsf{T}}+\frac{\beta_{\mathsf{T}}}{2}} e^{j\pi(n_1-n_2)\cos(\theta)}d\theta & \text{if } \beta_{\mathsf{T}}>0 \\ e^{j\pi(n_1-n_2)\cos(\overline{\theta}_{\mathsf{T}})} & \text{if } \beta_{\mathsf{T}}=0.\end{cases}$$

If $\{N_{\mathsf{tx}}, N_{\mathsf{tz}}\}\to\infty$ and $m_1-m_2\neq 0$ is such that it satisfies

$$\pi\cdot\min\left(\sin\left(\overline{\theta}_{\mathsf{T}}-\frac{\beta_{\mathsf{T}}}{2}\right),\ \sin\left(\overline{\theta}_{\mathsf{T}}+\frac{\beta_{\mathsf{T}}}{2}\right)\right)\cdot\sin\left(\frac{\alpha_{\mathsf{T}}}{2}\right)\cdot|m_1-m_2|\gg 1,$$

we have

$$\frac{\mathbf{R}_{\mathsf{tx}}(k_1,k_2)}{N_r} \approx \sqrt{\frac{2}{\alpha_{\mathsf{T}}^2\cdot(m_1-m_2)}}\cdot\mathsf{X}+\varepsilon, \tag{11}$$

where X is given in (12) *and the error term satisfies $\varepsilon = \mathcal{O}\left(\frac{1}{|m_1-m_2|}\right)$. On the receive side, as $\{N_{\mathsf{rx}}, N_{\mathsf{rz}}\}\to\infty$, we can approximate $\mathbf{R}_{\mathsf{tx}}$ with* (13)*, with the error term satisfying $\varepsilon = \mathcal{O}\left(\frac{1}{|m_1-m_2|^2}\right)$.*

Proof. Note that $E_0^+(w,z)\to\frac{2w}{\pi}$ as $z\to 0$ with continuity. Thus, we have the expression in (11) as in the statement of the proposition for the two cases: $\beta_{\mathsf{T}}>0$ and $\beta_{\mathsf{T}}=0$.

$$\frac{\mathbf{R}_{\mathsf{tx}}(k_1,k_2)}{N_r} = \int_{\theta\in\Theta_{\mathsf{T}}}\Big[F_1\Big(\pi(m_1-m_2)\sin(\theta)\Big)+jF_{2,\mathsf{T}}\Big(\pi(m_1-m_2)\sin(\theta)\Big)\Big]\cdot e^{j\pi(n_1-n_2)\cos(\theta)}g_{\mathsf{T}}(\theta)\ d\theta \tag{9}$$

$$\mathsf{X} = \begin{cases} \frac{1}{\beta_{\mathsf{T}}} \cdot \int_{\overline{\theta}_{\mathsf{T}}-\frac{\beta_{\mathsf{T}}}{2}}^{\overline{\theta}_{\mathsf{T}}+\frac{\beta_{\mathsf{T}}}{2}} \frac{e^{j\pi\left((m_1-m_2)\sin(\theta)+(n_1-n_2)\cos(\theta)-\frac{1}{4}\right)}}{\sqrt{\sin(\theta)}} d\theta & \text{if } \beta_{\mathsf{T}} > 0 \\ \frac{e^{j\pi\left((m_1-m_2)\sin(\overline{\theta}_{\mathsf{T}})+(n_1-n_2)\cos(\overline{\theta}_{\mathsf{T}})-\frac{1}{4}\right)}}{\sqrt{\sin(\overline{\theta}_{\mathsf{T}})}} & \text{if } \beta_{\mathsf{T}} = 0 \end{cases} \tag{12}$$

$$\frac{\mathbf{R}_{\mathsf{rx}}(k_1,k_2)}{N_t} = \frac{2\left[\sin\left(\pi\sqrt{(m_1-m_2)^2+(n_1-n_2)^2}\right)+\cos\left(\pi(n_1-n_2)\right)\right]}{\pi^2\cdot|m_1-m_2|} + \varepsilon. \tag{13}$$

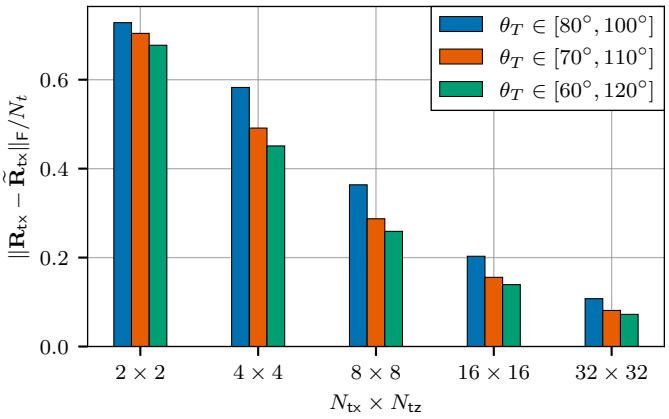

Fig. 1. Approximation accuracy for increasing UPA dimensions and different sectoral area coverages. As Prop. 3 predicts, the relative error decreases as the UPA dimensions $\{N_{\mathsf{tx}}, N_{\mathsf{tz}}\}$ increase.

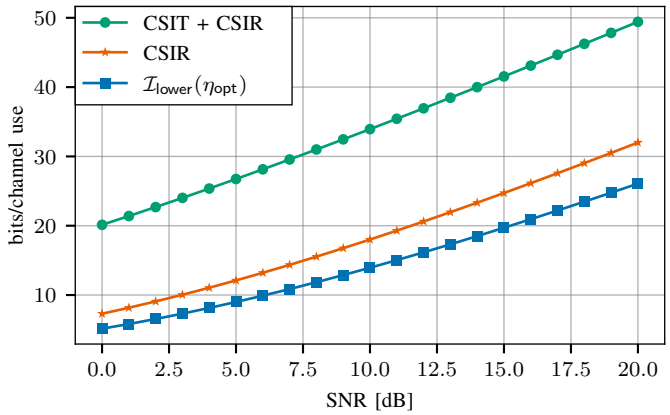

Fig. 2. Mutual information with channel information at both ends (labeled *CSIT+CSIR*), only at the receiver (labeled *CSIR*) and with the lower bound (17) for η_{opt} as $P \to \infty$. Model parameters: $\theta_{\mathsf{T}} \in [70°, 110°]$, $N_{\mathsf{tx}} = 8$, $N_{\mathsf{tz}} = 8$, $N_{\mathsf{rx}} = 4$, $N_{\mathsf{rz}} = 4$, $L = 5$, $N_{\mathsf{s}}/N_t = 10$

For the behavior of $\mathbf{R}_{\mathsf{tx}}(k_1,k_2)$ as $|k_1-k_2|$ increases with $\{N_{\mathsf{tx}}, N_{\mathsf{tz}}\} \to \infty$, from [18, 10.15, p. 69], note that

$$E_0^+(w,z) \approx \sqrt{\frac{2}{\pi z}} e^{j(z-\pi/4)} + \frac{2j\cdot e^{jz\cos(w)}}{\pi z \sin(w)} + \mathcal{O}\left(\frac{1}{z^{3/2}}\right)$$

if $|z\sin(w)| \gg 1$. Thus, we have (11) in the statement of the proposition. For the receive side, we note that [19, 9.2.1]

$$J_0(z) \overset{z\to\infty}{\to} \sqrt{\frac{2}{\pi z}} \cos\left(z-\frac{\pi}{4}\right) + \mathcal{O}\left(\frac{1}{z}\right),$$

which results in the expression in (13). ■

IV. Numerical Studies and Applications

This section presents numerical studies and simulation results using the derived exact and approximate expressions. We begin by investigating the accuracy of the approximation presented in Prop. 3 and follow this up with an investigation on the trade-off between data transmission and channel estimation when using the optimal sounding beams derived in Sec. III.

A. Transmit Covariance Approximation Accuracy

Fig. 1 studies the accuracy of the approximations from Prop. 3 for varying sector area coverages. More specifically, for varying uniform planar array (UPA) dimensions and sector widths, we let $\mathbf{R}_{\mathsf{tx}}$ be the exact expression from (5) and let $\widetilde{\mathbf{R}}_{\mathsf{tx}}$ be the approximation from Prop. 3. We observe that the overall trend of increased accuracy for increasing antenna dimensions holds even at the relatively small dimensions shown in the figure. This suggests that for sufficiently large antenna arrays, the use of the approximate expressions, which do not require the computation of special functions, is sufficient for further analysis and the development of adaptive algorithms.

B. Bounds on Mutual Information

To highlight an application of the expressions derived in this paper, we investigate the effect on the mutual information of the trade-off between channel estimation and data transmission when operating under a fixed energy budget. To illustrate this, we assume the traditional *channel estimation followed by data transmission* framework [12]–[15] and a fixed energy budget (over a channel coherence interval N_{s}) of PN_s, of which we allocate a fraction $\eta \in (0,1)$ for channel estimation and the remaining $(1-\eta)$ fraction for data transmission. The observation model during the channel estimation phase is thus

$$\mathbf{Y}_{\mathsf{tr}} = \sqrt{\frac{\eta P N_{\mathsf{s}}}{N_t}} \mathbf{H}\mathbf{X}_{\mathsf{tr}} + \mathbf{N}_{\mathsf{tr}} \tag{14}$$

whereas the input-output model during the data transmission is given as

$$\mathbf{y}_{\mathsf{si}} = \sqrt{\frac{(1-\eta)PN_{\mathsf{s}}}{(N_{\mathsf{s}}-N_t)N_t}} \mathbf{H}\mathbf{x}_{\mathsf{si}} + \mathbf{n}_{\mathsf{si}} \tag{15}$$

$$= \sqrt{\frac{(1-\eta)PN_{\mathsf{s}}}{(N_{\mathsf{s}}-N_t)N_t}} \widehat{\mathbf{H}}\mathbf{x}_{\mathsf{si}} + \mathbf{n}'_{\mathsf{si}}, \tag{16}$$

where

$$\mathbf{n}'_{\mathsf{si}} = \sqrt{\frac{(1-\eta)PN_{\mathsf{s}}}{(N_{\mathsf{s}}-N_t)N_t}} \left(\mathbf{H}-\widehat{\mathbf{H}}\right)\mathbf{x}_{\mathsf{si}} + \mathbf{n}_{\mathsf{si}}.$$

By treating the channel estimation error as noise [12], we arrive at a lower bound for the instantaneous mutual information in the form of

$$\mathcal{I} \geq \tfrac{N_{\mathsf{s}}-N_t}{N_{\mathsf{s}}} \cdot \log\det\left(\mathbf{I}_{N_r} + \tfrac{(1-\eta)PN_{\mathsf{s}}}{(N_{\mathsf{s}}-N_t)N_t} \cdot \widehat{\mathbf{H}}\widehat{\mathbf{H}}^{\dagger} \cdot \mathbf{\Sigma}_{\mathsf{n}}^{-1}\right), \quad (17)$$

where $\mathbf{\Sigma}_n = \mathcal{E}\left[\mathbf{n}'_{\mathsf{si}}\mathbf{n}'^{*}_{\mathsf{si}}\right]$ and the MMSE channel estimator $\widehat{\mathbf{H}}$ is defined as

$$\widehat{\mathbf{H}} = \sqrt{\frac{\eta PN_{\mathsf{s}}}{N_t}}\mathbf{Y}_{\mathsf{tr}}\left(\frac{\eta PN_s}{N_t}\mathbf{X}^*_{\mathsf{tr}}\mathbf{R}_{\mathsf{tx}}\mathbf{X}_{\mathsf{tr}} + \mathbf{I}_{N_t}\right)^{-1}\mathbf{X}^*_{\mathsf{tr}}\mathbf{R}_{\mathsf{tx}}.$$

We are now interested in understanding the optimal η as a function of transmit power P. Prop. 4 (proof omitted due to lack of space) outlines some asymptotic results.

Proposition 4. *As $P \to 0$, we have*

$$\eta_{\mathsf{opt}}(P) \to \frac{1}{2}. \quad (18)$$

Conversely, as $P \to \infty$, we have

$$\eta_{\mathsf{opt}}(P) \to \frac{\sqrt{N_t}}{\sqrt{N_{\mathsf{s}}-N_t}+\sqrt{N_t}}. \quad (19)$$

Fig. 2 compares (17) using the high-SNR η_{opt} from Prop. 4 against the ergodic capacity with perfect channel state information (CSI) at both the transmitter and receiver (waterfilling solution over the left and right singular vectors) and with perfect CSI at the receiver alone (with equi-power identity optimal signal covariance matrix). As we expect, given our derivation of the optimal sounding beams $\mathbf{X}_{\mathsf{tr}}$, the trend of the achievable scheme with η_{opt} tracks the trend seen with the perfect CSI at the receiver. We note that the value for η_{opt} used in this simulation is strictly sub-optimal for the lower SNR regime, which implies room additional performance gains with the non-asymptotic optimal $\eta_{\mathsf{opt}}(P)$.

V. Conclusion

We considered beam training over a generalized Saleh-Valenzuela mmW channel model in this work. This framework considers a channel estimation phase followed by data transmission and has been explored in prior work for sub-6 GHz frequencies. But to the best of our understanding, such a study at mmW frequencies is novel. Falling out of the structure of the optimal signaling matrices over the channel training phase is the need to understand the transmit covariance matrix of the channel. Towards this goal, we presented exact and approximate expressions for the transmit and receive covariance matrices with the mmW channel model. Numerical simulations studied the accuracy of the proposed approximations for varying system parameters. We finally presented preliminary results of our investigations on the achievable rates with the channel estimation–data transmission trade-off for a fixed energy budget over a single coherence interval. Our results show that the general rate trends realized with the achievable scheme are comparable to the trends realized assuming perfect channel state information at the receiver.

References

[1] F. Khan and Z. Pi, "An introduction to millimeter wave mobile broadband systems," *IEEE Commun. Magaz.*, vol. 49, no. 6, pp. 101–107, June 2011.

[2] E. Torkildson, U. Madhow, and M. Rodwell, "Indoor millimeter wave MIMO: Feasibility and performance," *IEEE Trans. Wireless Commun.*, vol. 10, no. 12, pp. 4150–4160, Dec. 2011.

[3] T. S. Rappaport, S. Sun, R. Mayzus, H. Zhao, Y. Azar, K. Wang, G. N. Wong, J. K. Schulz, M. K. Samimi, and F. Gutierrez, "Millimeter wave mobile communications for 5G cellular: It will work!," *IEEE Access*, vol. 1, pp. 335–349, 2013.

[4] W. Roh, J.-Y. Seol, J. Park, B. Lee, J. Lee, Y. Kim, J. Cho, K. Cheun, and F. Aryanfar, "Millimeter-wave beamforming as an enabling technology for 5G cellular communications: Theoretical feasibility and prototype results," *IEEE Commun. Magaz.*, vol. 52, no. 2, pp. 106–113, Feb. 2014.

[5] V. Raghavan, A. Partyka, S. Subramanian, A. Sampath, O. H. Koymen, K. Ravid, J. Cezanne, K. K. Mukkavilli, and J. Li, "Millimeter wave MIMO prototype: Measurements and experimental results," *IEEE Commun. Magaz.*, vol. 56, no. 1, pp. 202–209, Jan. 2018.

[6] V. Venkateswaran and A.-J. van der Veen, "Analog beamforming in MIMO communications with phase shift networks and online channel estimation," *IEEE Trans. Sig. Proc.*, vol. 58, no. 8, pp. 4131–4143, Aug. 2010.

[7] J. Brady, N. Behdad, and A. M. Sayeed, "Beamspace MIMO for millimeter-wave communications: System architecture, modeling, analysis and measurements," *IEEE Trans. Ant. Propagat.*, vol. 61, no. 7, pp. 3814–3827, July 2013.

[8] O. El Ayach, S. Rajagopal, S. Abu-Surra, Z. Pi, and R. W. Heath, Jr., "Spatially sparse precoding in millimeter wave MIMO systems," *IEEE Trans. Wireless Commun.*, vol. 13, no. 3, pp. 1499–1513, Mar. 2014.

[9] S. Hur, T. Kim, D. J. Love, J. V. Krogmeier, T. A. Thomas, and A. Ghosh, "Millimeter wave beamforming for wireless backhaul and access in small cell networks," *IEEE Trans. Commun.*, vol. 61, no. 10, pp. 4391–4403, Oct. 2014.

[10] V. Raghavan, J. Cezanne, S. Subramanian, A. Sampath, and O. H. Koymen, "Beamforming tradeoffs for initial UE discovery in millimeter-wave MIMO systems," *IEEE Journ. Sel. Topics in Sig. Proc.*, vol. 10, no. 3, pp. 543–559, Apr. 2016.

[11] V. Raghavan, S. Subramanian, J. Cezanne, A. Sampath, O. H. Koymen, and J. Li, "Single-user vs. multi-user precoding for millimeter wave MIMO systems," *IEEE Journ. Sel. Areas in Commun.*, vol. 35, no. 6, pp. 1387–1401, June 2017.

[12] M. Medard, "The effect upon channel capacity in wireless communications of perfect and imperfect knowledge of the channel," *IEEE Trans. Inform. Theory*, vol. 46, no. 3, pp. 935–946, May 2000.

[13] L. Zheng, D. N. C. Tse, and M. Medard, "Channel coherence in the low-SNR regime," *IEEE Trans. Inform. Theory*, vol. 53, no. 3, pp. 976–997, Mar. 2007.

[14] V. Raghavan, G. Hariharan, and A. M. Sayeed, "Capacity of sparse multipath in the ultraWideband regime," *IEEE Journ. Sel. Topics in Sig. Proc.*, vol. 1, no. 3, pp. 357–371, Oct. 2007.

[15] G. Hariharan, V. Raghavan, and A. M. Sayeed, "Capacity of sparse wideband channels with partial channel feedback," *Transactions on Emerging Telecommunications Technologies*, vol. 19, no. 4, pp. 475–493, June 2008.

[16] A. A. M. Saleh and R. Valenzuela, "A statistical model for indoor multipath propagation," *IEEE Journ. Sel. Areas in Commun.*, vol. 5, no. 2, pp. 128–137, Feb. 1987.

[17] C. A. Balanis, *Antenna Theory: Analysis and Design*, Wiley-Interscience, 3rd edition, 2005.

[18] M. M. Agrest and M. S. Maksimov, *Theory of Incomplete Cylindrical Functions and their Applications (Translated from Russian by H. E. Fettis, J. W. Goresh and D. A. Lee)*, Springer-Verlag, Berlin, 1971.

[19] M. Abramowitz and I. A. Stegun, *Handbook of Mathematical Functions with Formulas, Graphs and Mathematical Tables*, National Bureau of Standards, USA, 10th edition, 1972.

[20] A. Michaely, "Asymptotic analysis of edge-excited currents on a convex face of a perfectly conducting wedge under overlapping penumbra region conditions," *IEEE Trans. Ant. Propagat.*, vol. 44, no. 1, pp. 97–101, Jan. 1996.

[21] S. L. Dvorak, "Applications for incomplete Lipschitz-Hankel integrals in electromagnetics," *IEEE Ant. Propagat. Magaz.*, vol. 36, no. 6, pp. 26–32, Dec. 1994.